Supporting Information

A Metal-free Molecular Pyroelectric Material with Strong Pyro-Photovoltaic Coupling for Enhancing Self-Powered X-ray Response

Huaimin Ni[ab], Haojie Xu[ab], Aijun Liu[a], Wuqian Guo[a], Qingshun Fan[ab], Yi Liu[a]*, Zihao Zhao[ab], Xianmei Zhao[a], Junhua Luo[abc], and Zhihua Sun[abc]*

a. State Key Laboratory of Functional Crystals and Devices Fujian Institute of Research on the Structure of Matter Chinese Academy of Sciences Fuzhou, Fujian 350002, (P. R. China)

b. University of Chinese Academy of Sciences Beijing 100049, (P. R. China)

c. Fujian Science & Technology Innovation Laboratory for Optoelectronic Information of China Fuzhou, Fujian, 350108 (P. R. China)

*Correspondence: liuyi@fjirsm.ac.cn, sunzhihua@fjirsm.ac.cn

Figure

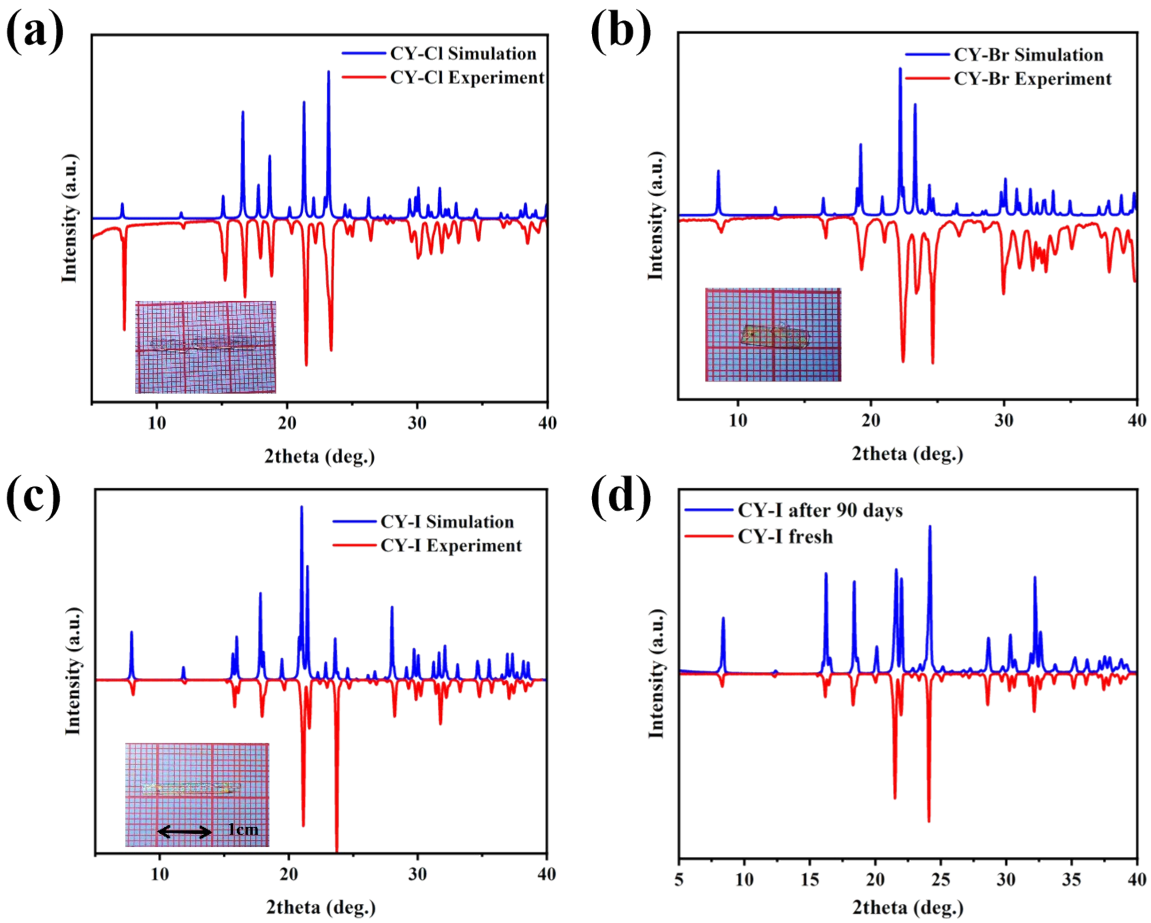

Figure S1. P-XRD patterns of simulation and experiment results of (a) **CY-Cl**, (b) **CY-Br**, and (c) **CY-I**, respectively (Insert: the bulk crystals), (d) Fresh and after 90 days P-XRD patterns of **CY-I** at room temperature.

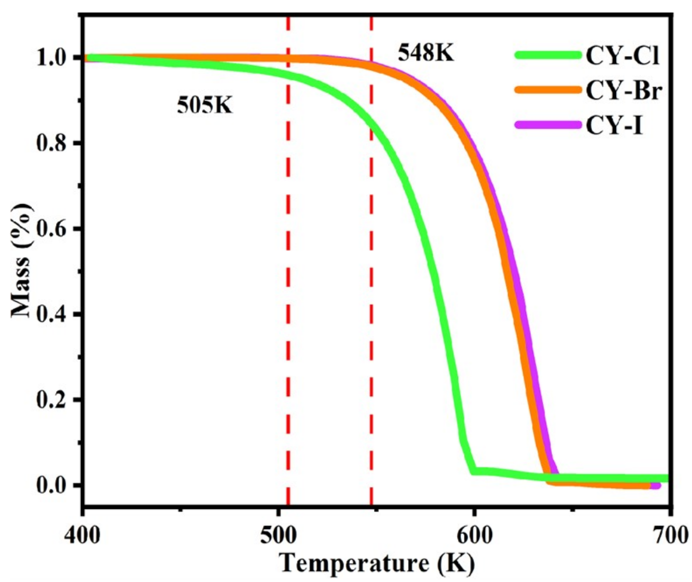

Figure S2. Thermal stability analysis of **CY-X**.

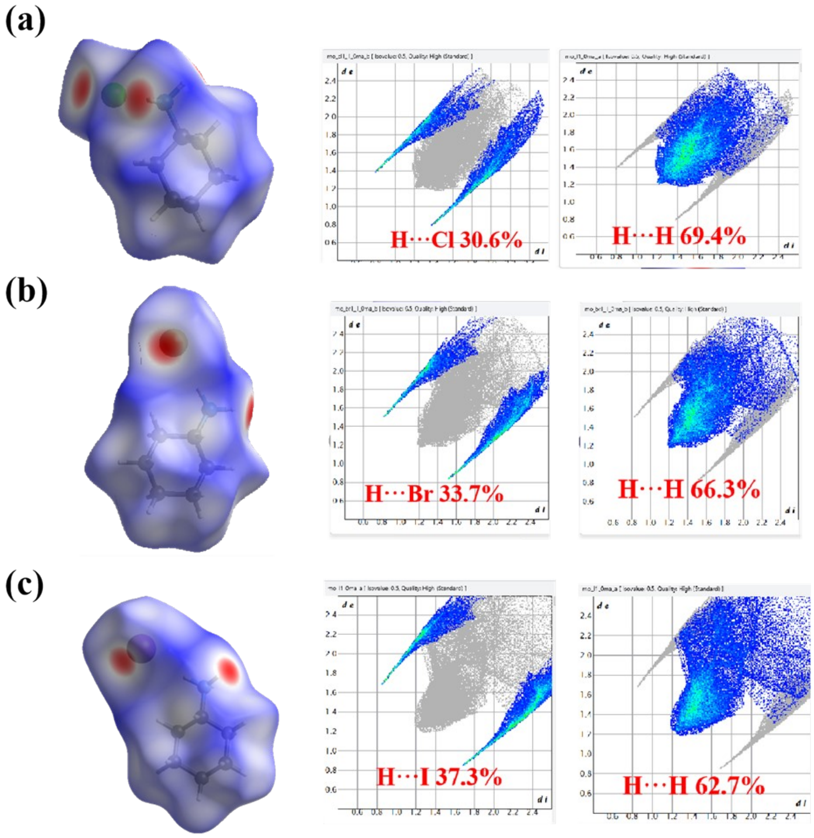

Figure S3. Hirshfeld d_{norm} surfaces and 2D finger plots of **CY-X**. (a) **CY-Cl**, (b) **CY-Br**, and (c) **CY-I**, respectively.

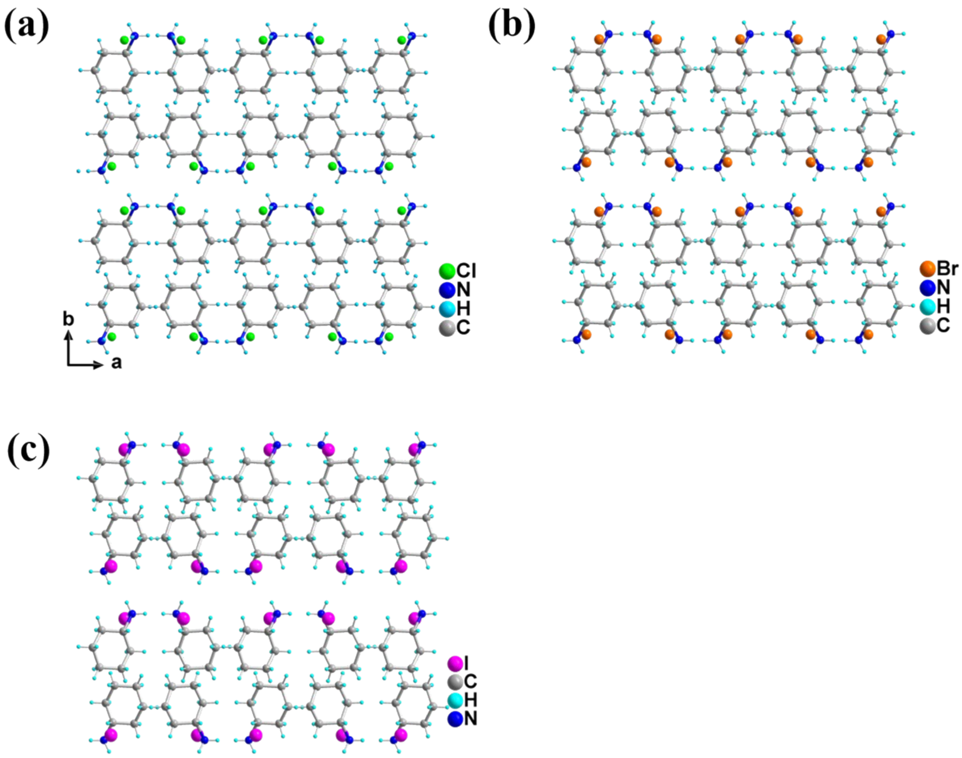

Figure S4. Stacking structures of **CY-X**. (a) **CY-Cl**, (b) **CY-Br**, and (c) **CY-I**, respectively.

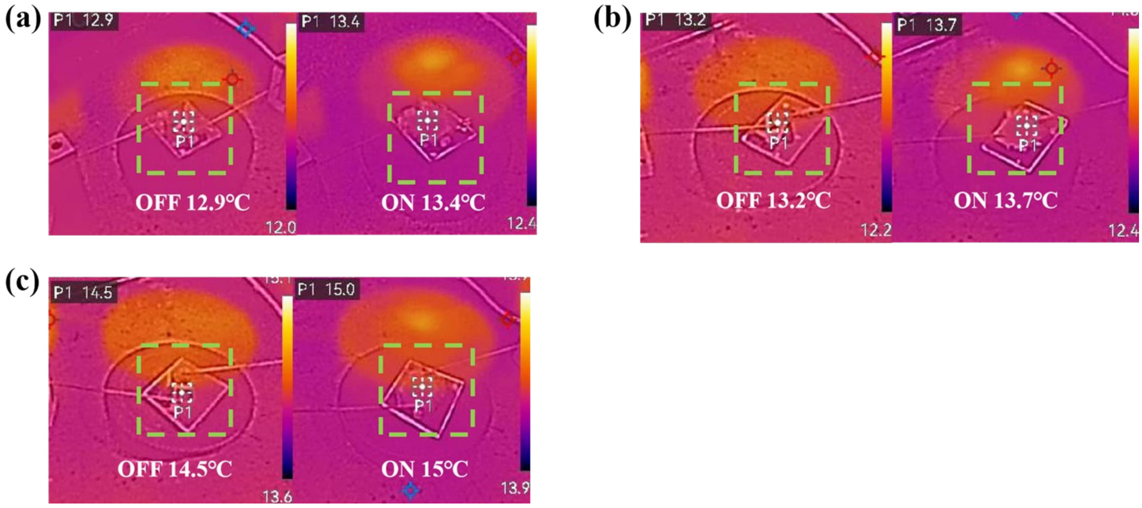

Figure S5. Light-induced temperature change on the crystal surface of (a) **CY-Cl**, (b) **CY-Br**, and (c) **CY-I**, respectively (404 nm, 100 mW cm^{-2}).

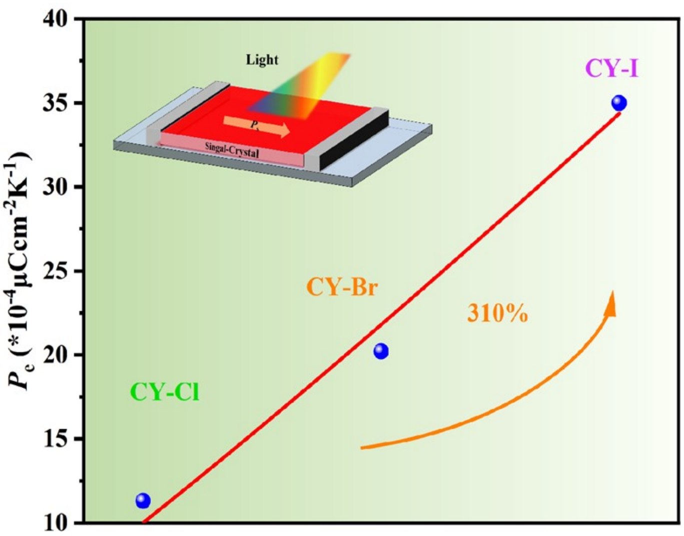

Figure S6. Comparison of pyroelectric properties (Insert: Single crystal-based photoexcited pyroelectric detectors).

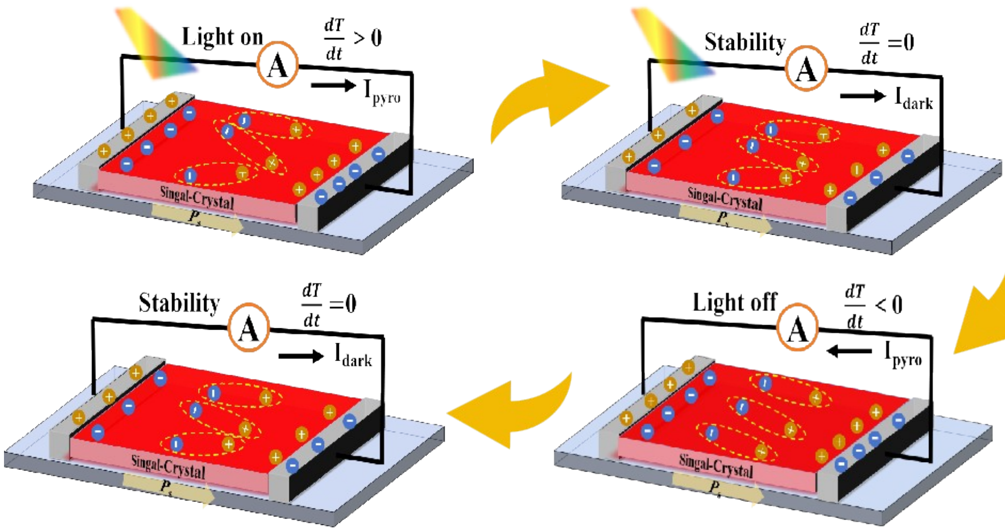

Figure S7. Illustration of the mechanism of the light-induced pyroelectric effects.

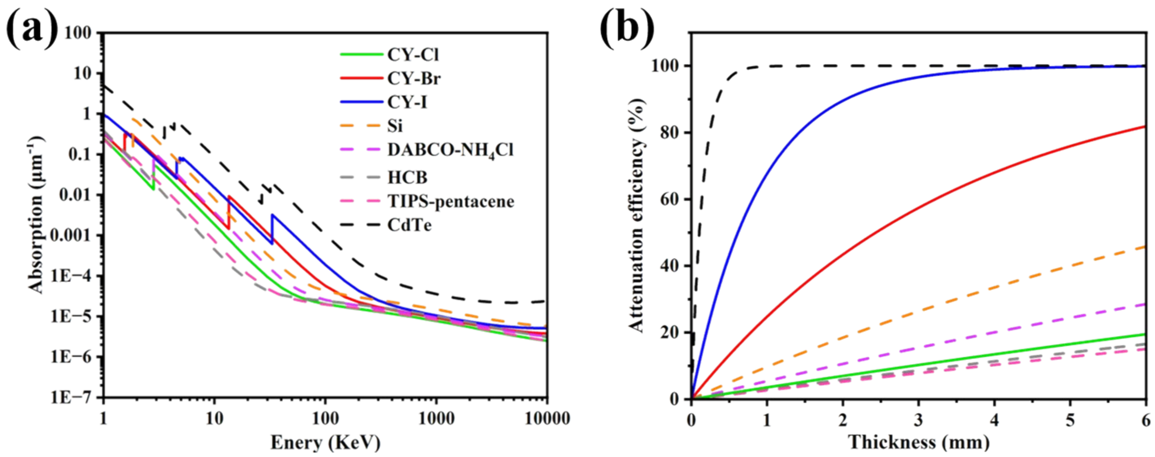

Figure S8. (a) Attenuation efficiency of **CY-X** and other representative semiconductors. (b) The absorption coefficients of **CY-X** and other representative semiconductors versus photon energy.

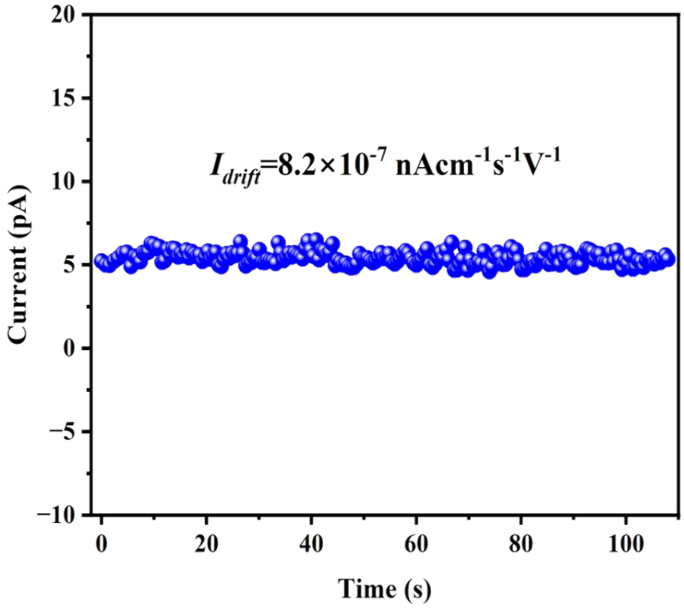

Figure S9. Dark current drift measurement of **CY-I** at 10 V_{bias}.

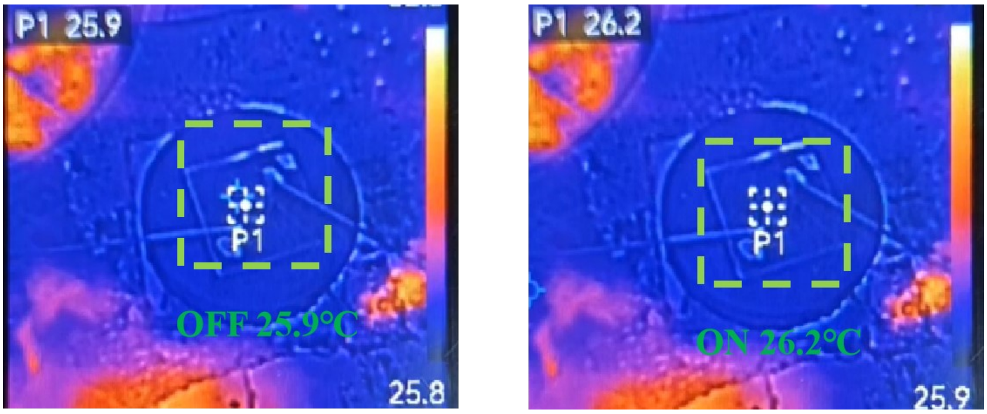

Figure S10. Thermal imaging photos of the crystal surface of **CY-I** in the dark and irradiated X-ray with 87.66 μGys^{-1}.

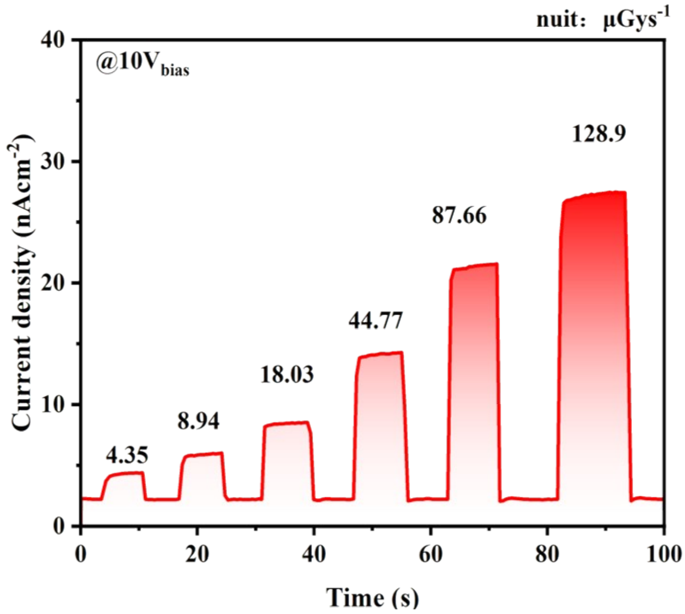

Figure S11. *I*-*t* curves of **CY-I** under different X-ray dose rates at 10 V_{bias}.

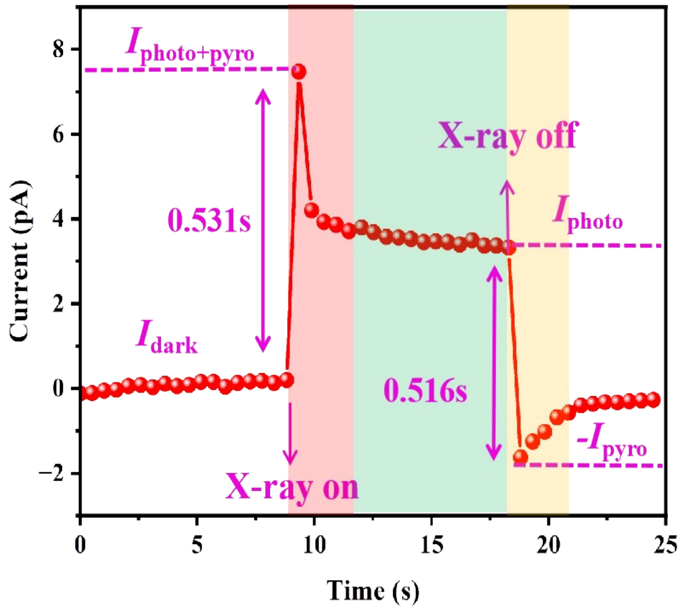

Figure S12. A representative different stage of the pyro-photovoltaic coupling effect under X-ray radiation.

Table

Table S1. Performance comparison of several broadband photodetectors.

Compound	Metal	Wavelength (nm)	Bias(V)	Ref
$(BDA)SbBr_5$	Sb-based	377-980	0	[1]
$(HDA)BiI_5$	Bi-based	X-ray, 377-980	0	[2]
$(BBA)_2(EA)_2Pb_3Br_{10}$	Pb-based	377-1950	0	[3]
$(NPA)_2(EA)_2Pb_3Br_{10}$	Pb-based	X-ray, 405-980	0	[4]
Multilayer WS_2	W-based	457-647	5	[5]
N-IBATFA	Metal-free	266-1950	0	[6]
CY-I	**Metal-free**	**X-ray, 266-980**	**0**	**This work**

Table S2. Performance comparison of several X-ray photodetectors.

Compound	Metal	Sensitivity ($\mu C\ Gy^{-1}\ cm^{-2}$)	Detection limit ($nGy\ s^{-1}$)	Bias(V)	Ref
P3HT:PCBM	Pb-based	83.53	1160	2	[4]
$(DGA)PbI_4$	Pb-based	4869	95.4	60	[7]
$HPIP_2$-NH_4I_5	Metal-free	81.7	12.2	10	[8]
DABCO-NH_4I_3	Metal-free	567	—	5	[9]
P_3HSe: $PC_{70}BM$	Metal-free	0.6	—	10	[10]
CY-I	**Metal-free**	**88**	**137**	**0**	**This work**

Table S3. Performance comparison of several self-powered X-ray photodetectors.

Compound	Metal	Sensitivity	Detection limit (nGy s^{-1})	Bias(V)	Ref
$(HDA)BiI_5$	Bi-based	171.7 μC Gy^{-1} cm^{-2}	266	0	[2]
$(NPA)_2(EA)_2Pb_3Br_{10}$	Pb-based	225 μC Gy^{-1} cm^{-2}	83.4	0	[4]
$FAPbBr_3$	Pb-based	7.28 C Gy^{-1} cm^{-3}	133	0	[11]
$CsPbI_2Br$	Pb-based	1.2 C Gy^{-1} cm^{-3}	25.69	0	[12]
$CH_3NH_3PbI_3$	Pb-based	25 μC mGy^{-1} cm^{-3}	—	0	[13]
CY-I	**Metal-free**	**88 μC Gy^{-1} cm^{-2}**	**137**	**0**	**This work**

Table S4. Crystal data and structure refinement **CY-X**.

Empirical formula	$C_6H_{14}ClN$	$C_6H_{14}BrN$	$C_6H_{14}IN$
Formula weight	135.63	180.09	227.089
Temperature/K	230.00	230.00	230.00
Crystal system	orthorhombic	orthorhombic	orthorhombic
Space group	$Pca2_1$	$Pca2_1$	$Pca2_1$
a/Å	9.3244(8)	9.557(3)	9.960(2)
b/Å	11.4638(9)	11.248(3)	11.304(2)
c/Å	7.5517(4)	7.849(3)	8.2803(16)
α/°	90	90	90
β/°	90	90	90
γ/°	90	90	90
Volume/Å^3	807.22(10)	843.7(4)	932.3(3)
Z	4	4	4
ρ_{calcg}/cm^3	1.116	1.418	1.618
μ/mm^{-1}	0.384	4.787	3.358
F(000)	296.0	368.0	438.6
Radiation	Mo Kα (λ = 0.71073)	Mo Kα (λ = 0.71073)	Mo Kα (λ = 0.71073)
2Θ range for data collection/°	5.632 to 54.934	5.594 to 50.022	5.46 to 50.02
Index ranges	$-11 \le h \le 12$, $-13 \le k \le 14$, $--9 \le l \le 9$	$-11 \le h \le 11$, $-13 \le k \le 14$, $--9 \le l \le 9$	$-12 \le h \le 12$, $-14 \le k \le 14$, $--10 \le l \le 10$
Reflections collected	5466	2846	4823
Independent reflections	1840 [R_{int} = 0.0657, R_{sigma} = 0.0661]	1339 [R_{int} = 0.0994, R_{sigma} = 0.1247]	1473[R_{int} = 0.0630, R_{sigma} = 0.0689]
Data/restraints/parameters	1840/1/75	1339/120/75	1473/120/75
Goodness-of-fit on F^2	1.038	1.576	1.747
Final R indexes [I>=2σ (I)]	R_1 = 0.0461, wR_2 = 0.0945	R_1 = 0.1250, wR_2 = 0.2587	R_1 = 0.1011, wR_2 = 0.2514
Final R indexes [all data]	R_1 = 0.0747, wR_2 = 0.1106	R_1 = 0.1976, wR_2 = 0.3009	R_1 = 0.1102, wR_2 = 0.2617
Largest diff. peak/hole/eÅ^{-3}	0.18/-0.19	0.88/-0.90	1.02/-2.49

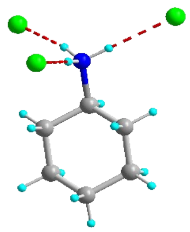

Table S5. Bond lengths for **CY-Cl** at 230 K.

Atom	Atom	Length/Å	Atom	Atom	Length/Å
N002	C003	1.503(5)	C005	C007	1.516(6)
C003	C004	1.508(6)	C006	C007	1.516(6)
C003	C005	1.504(5)	C006	C008	1.516(6)
C004	C008	1.517(7)			

Table S6. Bond angles for **CY-Cl** at 230 K.

Atom	Atom	Atom	Angle/˚	Atom	Atom	Atom	Angle/˚
N002	C003	C004	110.0(4)	C003	C005	C007	111.2(4)
N002	C003	C005	110.5(3)	C008	C006	C007	111.6(4)
C005	C003	C004	112.3(3)	C005	C007	C006	111.5(4)
C003	C004	C008	111.0(4)	C006	C008	C004	110.9(4)

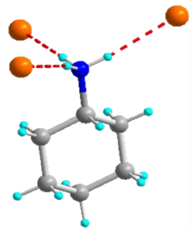

Table S7. Bond lengths for **CY-Br** at 230 K.

Atom	Atom	Length/Å	Atom	Atom	Length/Å
N002	C003	1.485(12)	C005	C008	1.509(12)
C003	C004	1.497(12)	C006	C007	1.505(12)
C003	C005	1.507(13)	C007	C008	1.506(12)
C004	C006	1.506(12)			

Table S8. Bond angles for **CY-Br** at 230 K.

Atom	Atom	Atom	Angle/˚	Atom	Atom	Atom	Angle/˚
N002	C003	C004	114.1(11)	C003	C005	C008	111.5(11)
N002	C003	C005	112.7(12)	C007	C006	C004	112.0(12)
C004	C003	C005	113.4(17)	C006	C007	C008	112.4(11)
C003	C004	C006	112.5(12)	C007	C008	C005	111.9(12)

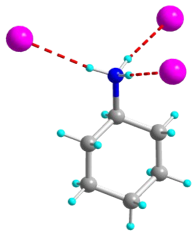

Table S9. Bond lengths for **CY-I** at 230 K.

Atom	Atom	Length/Å	Atom	Atom	Length/Å
C10	C11	1.501(8)	C006	C00A	1.507(8)
C10	N005	1.508(8)	C007	C009	1.516(8)
C10	C006	1.488(9)	C009	C00A	1.518(8)
C11	C007	1.503(8)			

Table S10. Bond angles for **CY-I** at 230 K.

Atom	Atom	Atom	Angle/°	Atom	Atom	Atom	Angle/°
N005	C10	C11	112.0(7)	C00A	C006	C10	112.7(8)
C006	C10	C11	111.9(11)	C009	C007	C11	111.6(8)
C006	C10	N005	112.8(9)	C00A	C009	C007	111.1(7)
C007	C11	C10	112.2(8)	C009	C00A	C006	111.7(8)

References

1. Y. Wang, H. Ye, P. Wang, Z. Wu, Q. Guan, C. Zhang, H. Li, S. Chen and J. Luo, *Adv. Mater*. 2024, **36**, e409245.
2. D. Fu, Y. Ma, S. Wu, L. Pan, Q. Wang, R. Zhao, X. M. Zhang and J. Luo, *InfoMat*, 2024, **6**, e12602.
3. L. Tang, W. Weng, H. Chen, L. Hua, W. Guo, Y. Liu, Y. Ma, Y. Chen, J. Luo and Z. Sun, *Adv. Funct. Mater.* 2023, **33**, 2214858.
4. Y. Ma, W. Li, Y. Liu, W. Guo, H. Xu, S. Han, L. Tang, Q. Fan, J. Luo and Z. Sun, *ACS Cent. Sci.* 2023, **9**, 2350-2357.
5. N. Perea-López, A. L. Elías, A. Berkdemir, A. Castro-Beltran, H. R. Gutiérrez, S. Feng, R. Lv, T. Hayashi, F. López-Urías, S. Ghosh, B. Muchharla, S. Talapatra, H. Terrones and M. Terrones, *Adv. Funct. Mater.* 2013, **23**, 5511-5517.
6. X. Zeng, Y. Liu, W. Weng, L. Hua, L. Tang, W. Guo, Y. Chen, T. Yang, H. Xu, J. Luo and Z. Sun, *Nat. Commun*. 2023, **14**, 5821.
7. B. Zhang, T. Zheng, J. You, C. Ma, Y. Liu, L. Zhang, J. Xi, G. Dong, M. Liu and S. Liu, *Adv. Mater.* 2022, **35**, e2208875.
8. P. Dong, C. Lin, N. Ye and M. Luo, *Angew. Chem. Int. Ed*.2024, **63**, e202407048.
9. Q. Cui, X. Song, Y. Liu, Z. Xu, H. Ye, Z. Yang, K. Zhao and S. Liu, *Matter*, 2021, **4**, 2490-2507.
10. M. P. A. Nanayakkara, Q. He, A. Ruseckas, A. Karalasingam, L. Matjacic, M. G. Masteghin, L. Basiricò, I. Fratelli, A. Ciavatti, R. C. Kilbride, S. Jenatsch, A. J. Parnell, B. Fraboni, A. Nisbet, M. Heeney, K. D. G. I. Jayawardena and S. R. P. Silva, *Adv. Sci.* 2023, **10**, e2304261.
11. M. Girolami, F. Matteocci, S. Pettinato, V. Serpente, E. Bolli, B. Paci, A. Generosi, S. Salvatori, A. Di Carlo and D. M. Trucchi, *Nano-Micro Lett.* 2024, **16**, 182.
12. P.-T. Lai, H.-C. Lin, Y.-T. Chuang, C.-Y. Chen, W.-K. Cheng, G.-H. Tan, B.-W. Hsu, L. Yang, S.-C. Lou, L.-J. Chien, H.-W. Wang and H.-W. Lin, *ACS Appl. Mater. Interfaces.* 2022, **14**, 19795-19805.
13. S. Yakunin, M. Sytnyk, D. Kriegner, S. Shrestha, M. Richter, G. J. Matt, H. Azimi, C. J. Brabec, J. Stangl, M. V. Kovalenko and W. Heiss, *Nat. Photonics*. 2015, **9**, 444-449.